A Nuclear Magnetic Resonance Study of the Solution Conformations of the Antibiotic Pseudomonic Acid A.†

Jeremy R. Everett* and John W. Tyler
Beecham Pharmaceuticals, Chemotherapeutic Research Centre, Brockham Park, Betchworth, Surrey RH3 7AJ

The proton and carbon n.m.r. spectra of pseudomonic acid A (**1**) were assigned by two-dimensional (2D) n.m.r. methods. The solution conformations of the tetrahydropyran (thp) ring, and some of the side-chain bonds of (**1**) and its sodium salt (**2**), were very similar to those of the antibacterially inactive monic acid A (**3**). Thus the inactivity of (**3**) is due to the lack of the nonanoic acid side-chain rather than any conformational changes. In D_2O both (**2**) and (**3**) were shown to populate a previously undetected thp ring conformation. The crystal structures of three compounds related to (**1**), (**2**), and (**3**) displayed only some of the conformations adopted by (**1**)—(**3**) in solution. It was concluded that there is a great potential for n.m.r. data as well as *X*-ray data to be used as input for computer modelling of molecular shape.

Pseudomonic acid A (**1**) is a naturally occuring antibiotic produced by fermentation of a strain of *Pseudomonas fluorescens*.[1] The structure (**1**) was elucidated[2,3] by degradative, spectroscopic, and *X*-ray work. However, although a few assignments of the ^1H n.m.r. spectrum of the methyl ester of (**1**) have been reported,[2,3] no complete analysis was made and no details of the ^1H n.m.r. spectrum of (**1**) itself have been published.

2D N.m.r. methods at high field have been used here to assign the complex, overlapped ^1H n.m.r. spectra of (**1**). Stereospecific coupling constants and nuclear Overhauser effects (n.O.e.s)[4] were then used to determine the solution conformations adopted by (**1**) and its sodium salt (**2**). These conformations were compared with those of monic acid (**3**) to determine whether the antibacterial inactivity of (**3**) was due to a conformational change in the molecule. The solution conformations of (**1**) and (**2**) were also compared with the crystalline-state conformations of three related compounds: ethyl 2-fluoromonate A, ethyl monate C, and a hydrazone of the nuclear ketone.

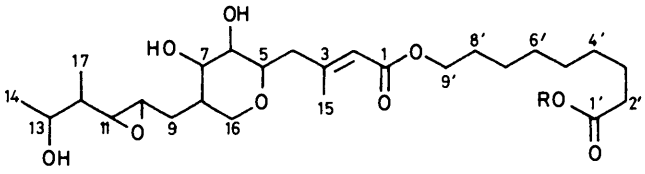

(**1**) R = H
(**2**) R = Na

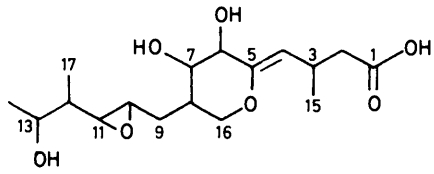

(**3**)

Results and Discussion

Table 1 gives all the proton and carbon n.m.r. chemical shifts, proton–proton couplings, and inter-proton n.O.e.s for (**1**). Table 2 compares the solution-state conformations of (**1**) and (**2**) with the crystalline-state conformations of related compounds.

Two-dimensional N.m.r. Spectroscopy.—As a prelude to the detailed interpretation of the n.m.r. spectra of (**1**), an unambiguous assignment of the resonances was required. A 2D chemical-shift-correlated[5,6] (SECSY) ^1H n.m.r. spectrum of (**1**) in CD_3OD is shown as a contour plot in Figure 1, below the normal one-dimensional (1D) ^1H spectrum. Connectivities between scalar-coupled protons are detected by the presence of symmetrical cross-peaks in the f1 dimension of the 2D spectrum. These cross-peaks occur at half the chemical shift difference between the coupled protons and they serve to identify mutually adjacent protons in the structure. Starting from the olefinic proton H-2, which may be unambiguously assigned to the signal at δ 5.73, connectivities can be seen (picked out in the Figure with bold diagonal lines) to both 4-protons and the C-15 methyl. Further connectivities may then be traced, in an unbroken sequence, all the way across the ring and down the epoxide side-chain to the C-14 methyl. In the nonanoic acid side-chain, connectivities are seen from 9′ to 8′ to 7′, and from 2′ to 3′ to 4′. Thus the only protons the chemical shifts of which cannot be unambiguously assigned are the 5′- and 6′-protons in the middle of the nonanoic acid side-chain.

A 2D $^{13}C,^1H$ correlation spectrum[7] of (**1**) in CD_3OD was then run in order to assign the ^{13}C n.m.r. spectrum. This 2D spectrum (shown as a contour plot in Figure 2) correlates the chemical shift of a proton with the chemical shift of the carbon to which it is directly bonded. For example the resonance of the protons of the C-17 methyl occurs at δ 0.94 in the proton n.m.r. spectrum (Figure 1). In the 2D $^1H,^{13}C$ correlation spectrum a cross-peak is seen at δ_H 0.94, δ_C 12.4 (Figure 2, top right-hand corner). This automatically and unambiguously assigns the carbon-13 resonance of the C-17 methyl at δ 12.4. The rest of the ^{13}C n.m.r. spectrum of (**1**) was assigned from the same 2D spectrum and these assignments are shown in Figure 2. The assignments agree with those of Feline *et al.*[8] for the methyl ester of (**1**) in $CDCl_3$ except that the order of C-7 and C-13 is reversed. This may be due to the different solvent used.

† The approved generic name for pseudomonic acid A is Mupirocin.

Table 1. Chemical shifts (δ),[a] coupling constants ($^nJ_{H,H}$/Hz), and inter-proton n.O.e.s for pseudomonic acid A

Atom	δ_C (CD_3OD)	s[c]	δ_H (CD_3OD)[b]	δ_H [$(CD_3)_2CO$]	$^nJ_{H,H}$ [$(CD_3)_2CO$]									$^1H,^1H$ n.O.e.s[e]							Atom
2	118.2	+	5.73	5.72													9′[f]	5		4*ax*	2
4*eq*	43.9	−	2.63	2.67	^2J 14.3	$^3J_{4,5}$	2.7				$^4J_{4,2}$	1.3	$^4J_{4,15}$ br[d]								4*eq*
4*ax*			2.21	2.22	^2J 14.3	$^3J_{4,5}$	9.5				$^4J_{4,2}$	0.8									4*ax*
5	76.3	+	3.73	3.69		$^3J_{5,4}$	9.4	$^3J_{5,4}$	2.6	$^3J_{5,6}$ 9.4							2	4*eq*		15	5
6	70.1	+	3.35	3.39		$^3J_{6,5}$	9.1	$^3J_{6,7}$	3.2												6
7	71.6	+	3.87	3.93		$^3J_{7,6}$	3.2	$^3J_{7,8}$	3.2		$^4J_{7,16}$	br[d]		6			10	11[f]		9b	7
8	41.5	+	*ca.* 1.93	*ca.* 1.97																	8
9a	33.1	−	1.70	1.72	^2J 14.1	$^3J_{9,8}$	7.7	$^3J_{9,10}$	6.1		$^4J_{9,16ax}$	0.3					16*eq*	6		11[f]	9a
9b			1.66	1.63	^2J 14.1	$^3J_{9,8}$	6.9	$^3J_{9,10}$	5.4								7	6		11	9b
10	56.9	+	2.81	2.79		$^3J_{10,9}$	5.8	$^3J_{10,9}$	5.8	$^3J_{10,11}$ 2.2				7	16*eq*	8	12		17	10
11	61.4	+	2.71	2.70		$^3J_{11,10}$	2.2	$^3J_{11,12}$	7.4					6	9a,b	14[f]	17[f]	7[f]	16*eq*[f]	11
12	43.7	+	*ca.* 1.41	1.39		$^3J_{12,11}$	7.2	$^3J_{12,13}$	4.9	$^3J_{12,17}$ 7.2											12
13	70.8	+	3.78	3.79		$^3J_{13,12}$	4.9	$^3J_{13,14}$	6.4												13
14	20.5	+	1.20	1.17		$^3J_{14,13}$	6.4										11		17[f]		14
15	19.5	+	2.18	2.19							$^4J_{15,2}$	1.3									15
16*ax*	66.4	−	3.84	3.84	^2J 11.4	$^3J_{16,8}$	2.8				$^4J_{16,9b}$	0.3									16*ax*
16*eq*			3.55	3.54	^2J 11.4	$^3J_{16,8}$	1.8				$^4J_{16,7}$	1.0					10	9a		11	16*eq*
17	12.4	+	0.94	0.92		$^3J_{17,12}$	7.1											10		11	17
2′	35.0	−	2.28	2.29		$^3J_{2'3'}$	7.3														2′
3′	26.1	−	*ca.* 1.60	1.7—1.5																	3′
4′	30.40	−	*ca.* 1.3	1.4—1.3																	4′
5′	30.26	−																			5′
6′	30.14	−																			6′
7′	27.0	−	1.36																		7′
8′	29.86	−	*ca.* 1.65	1.7—1.5																	8′
9′	64.9	−	4.06	4.05		$^3J_{9',8'}$	6.6														9′

[a] δ(Me_4Si) = 0. [b] From 2D ^1H SECSY spectrum; agreement with ^1H δ from 2D ^1H, ^{13}C correlation spectrum, 14 ± 10 p.p.b. [c] Sign of the signal in 63 MHz ^{13}C spin-echo spectrum. [d] Coupling unresolved: broad signal which sharpens on decoupling. [e] The entries in this column denote the proton at which an n.O.e. was *observed*. [f] Effect weak.

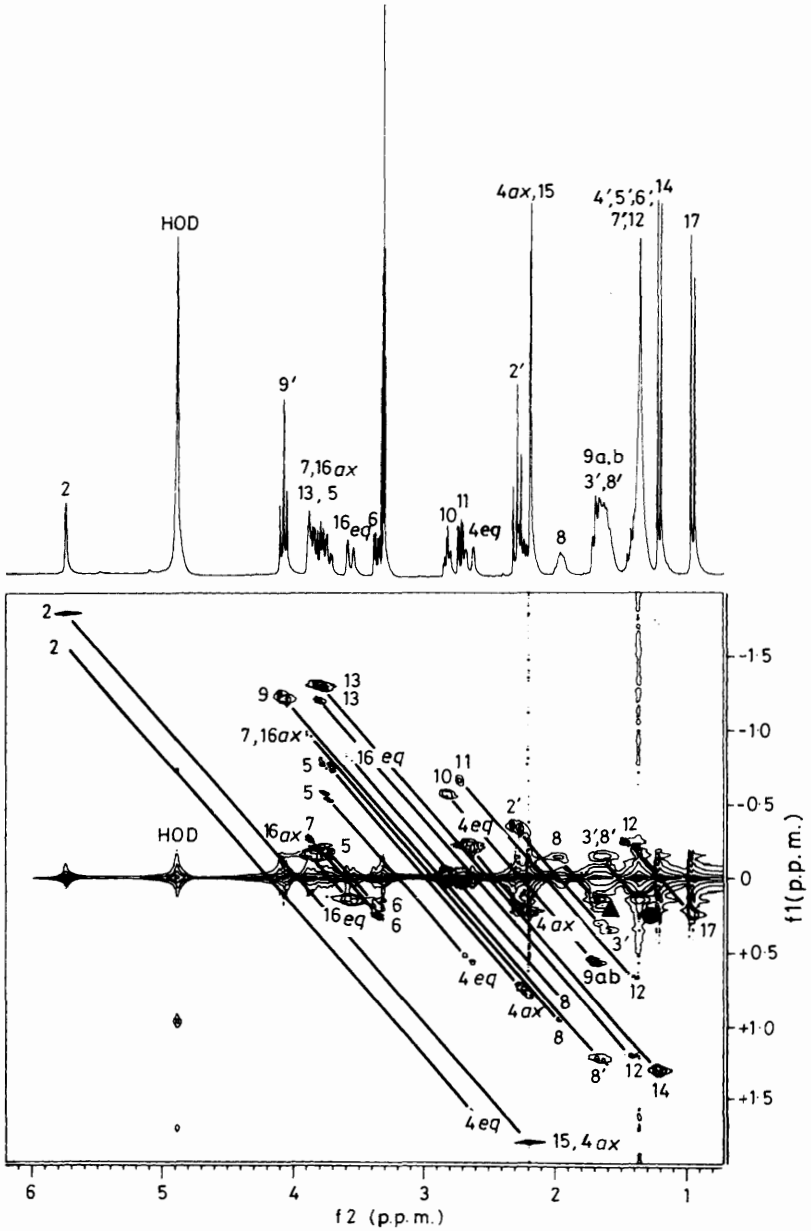

Figure 1. A contour plot of the 250 MHz 2D ^{1}H SECSY (45°, N-type) spectrum of pseudomonic acid A in CD_3OD. Connectivities between scalar-coupled protons are indicated by the bold diagonal lines linking the relevant cross-peaks. The cross-peak marked with a triangle (▲) is due to H-9a,9b and that marked with a circle (●) is due to H-4', H-7'. The conventional 1D ^{1}H n.m.r. spectrum is shown above the 2D spectrum

Conformational Analysis of Pseudomonic Acid A in [$^2H_6$]-*Acetone.*—The conformational analysis of (**1**) was based on the measurement of stereospecific inter-proton couplings and n.O.e.s. The magnitude of the n.O.e. depends upon an inverse sixth power proportionality of the distance between the two nuclei involved and is therefore an excellent probe of nuclear proximity and hence conformation.

This work was performed with [$^2H_6$]acetone solutions, as it proved impossible to obtain all the required couplings from the overlapped proton spectrum in CD_3OD, even using 2D ^{1}H *J*-resolved n.m.r. spectroscopy. The ^{1}H n.m.r. spectrum of (**1**) in [$^2H_6$]acetone was easily solved with the CD_3OD data in hand.

The tetrahydropyran ring. The magnitudes of $^3J_{5,6}$, $^3J_{6,7}$, $^3J_{7,8}$, $^3J_{8,16ax}$, and $^3J_{8,16eq}$ allowed these couplings to be assigned as *ax,ax*, *ax,eq*, *eq,eq*, *eq,ax*, and *eq,eq*, respectively. Thus the tetrahydropyran (thp) ring was predominantly in the *C*1 conformation as expected.

The H-16*eq* signal was assigned on the basis of a stereospecific ^4J W coupling[9] to H-7 and is upfield of that due to H-16*ax* with a smaller coupling to H-8. The reverse assignment by Chain *et al.*[3] for the triacetate of the nuclear ketone appears to be incorrect.

Conformation of the 4,5-*bond.* The H-4*ax* signal was distinguished from that due to H-4*eq* by the magnitudes of $^3J_{5,4}$. The near maximal $^3J_{5,4ax}$ value indicated that there was little free rotation around the 4,5-bond. This correlates well with a recent study[10] of segmental motion in (**1**) which came to the same conclusion on the basis of ^{13}C relaxation times. The H-4*eq*

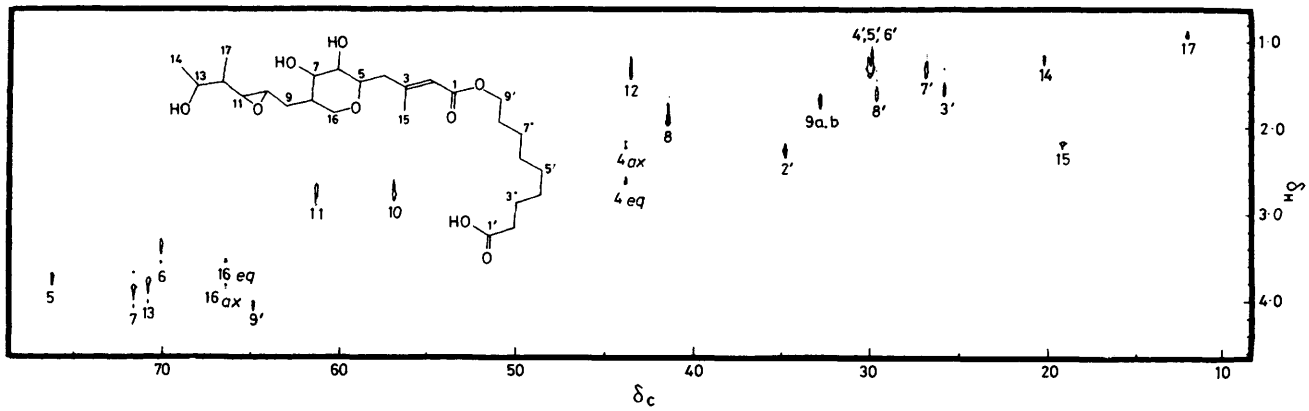

Figure 2. A contour plot of the 2D $^1H,^{13}C$ correlation spectrum of pseudomonic acid A in CD_3OD

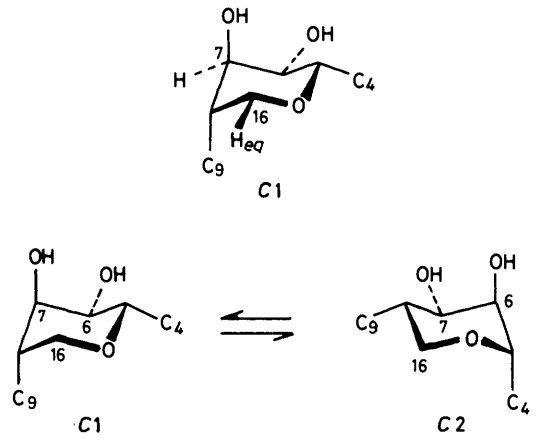

signal was assigned *trans*-coplanar to the thp oxygen on the basis of the low value of $^3J_{5,4eq}$.[11] Thus the conformation of the 4,5-bond is as shown in (A).

Conformations of the 3,4-*bond.* Figure 3 shows a control ^1H n.m.r. spectrum of (**1**) underneath a selection of n.O.e. difference spectra obtained after irradiation of the proton indicated (number in parentheses). Upon irradiation at the H-2 frequency n.O.e.s are seen at the H-5 (1.4%) and H-4*ax* signals (2.9%), indicating that H-2 is close in space to both these protons. Since H-5 and H-4*ax* are *trans*-diaxial, (**1**) must exist as a mixture of *two* conformations about the 3,4-bond, (B) and (C). In (B), H-2 is close to H-4*ax*; in (C) it is close to H-5. Further confirmation of the existence of the two conformations comes from the observation of n.O.e.s at the 15-H_3 (B) and H-2 (C) signals upon irradiation at the H-5 frequency (not shown).

The unlikely possibility of one or more skew conformations, like (*D*), giving rise to the n.O.e. results is eliminated by the observation of three long-range, four-bond couplings ($^4J_{2,4eq}$, $^4J_{2,4ax}$, and $^4J_{4eq,15}$). The coupling $^4J_{2,4eq}$ is greater than $^4J_{2,4ax}$, which implies[9] that H-2 is closer to coplanarity with H-4*ax* than with H-4*eq*. This coplanarity is achieved in (B) and (C) but not (D). The observation of a coupling between 15-H_3 and H-4*eq* but not H-4*ax* means[9] that H-4*eq* is able to overlap with a lobe of the π system on C-3. This is possible for (B) and (C) but not (D). Diagram (B′) shows how this overlap is achieved for conformation (B).

The 4*ax*-proton has a geminal partner which will provide most of its relaxation; H-5 has no such partner. Since the H-2 to H-5 and H-2 to H-4*ax* distances are similar in (C) and (B), respectively, a larger n.O.e. would be expected at H-5 upon irradiation at the frequency of H-2, if the populations of (B) and (C) were similar. Since this is not the case, (B) is the major and (C) the minor conformer about the 3,4-bond.

Conformations of the 8,9-*bond.* Upon irradiation at the frequency of H-16*ax* the eight lines of the H-9b signal all became narrower, showing the existence of an unresolved ^4J W coupling. The sharp lines of H-9a to low field showed no change. This experiment not only served to distinguish the 9-protons but showed that the 8,9-bond must populate conformer (E) with a W between H-9b and H-16*ax*.

However, conformation (E) cannot be the only one populated by the 8,9-bond. Irradiation at the frequency of H-9b gave an n.O.e. at H-6 as well as H-7. The 9b-proton is close to H-7 in (E) but can only become close to H-6 in (F). Further confirmation of the existence of (E) *and* (F) came from the observation of n.O.e.s at H-6 (E) and H-16*eq* (F) upon irradiation at the frequency of H-9a. These results were again confirmed by the observation of specific n.O.e.s to H-9a and 9b upon irradiation at the frequencies of H-16*eq* and H-7, respectively (Figure 3).

The two values of $^3J_{8,9}$ are time-averaged over (E) and (F). The larger value of $^3J_{8,9a}$ indicated that (E), with H-9a *trans* to H-8, was probably preferred over (F). It is very unlikely that (G) is populated at all, owing to severe steric repulsions. The existence of the two conformations (E) and (F) in equilibrium ties in with the observation[10] of a relatively large increase in motion from C-8 to C-9 in comparison with that from C-5 to C-4.

Conformations of the 9,10-*bond.* Irradiation at the frequency of H-10 gave n.O.e.s at H-7 and H-16*eq* (Figure 3), indicating that H-10 can be close to both these protons. This can only occur if the 8,9-bond adopts both conformations (E) and (F). The 10-proton can be close to H-7 and H-16*eq* in (F) and (E), respectively. Diagrams (E′) and (F′) show how this is achieved.

The populations of conformations (E′) and (F′) relative to others like (F″), with H-10 close to H-8 rather than H-7, were not determined. However, since irradiation of H-10 also gave an n.O.e. at H-8, conformers like (F″) and the equivalent (E″) (not shown) must be populated.

Since irradiations at the frequencies of H-7 and H-16*eq* both gave small n.O.e.s at H-11, it is also likely that conformations like (F‴) are populated.

The 7-proton is close to H-11 in (F‴) and H-16*eq* is close to H-11 in the equivalent (E‴) conformation (not shown). Conformations (F′), (F″), and (F‴) correspond roughly to the three staggered conformations of the 9,10-bond for the 8,9-bond conformation (F). Conformations (E′), (E″), and (E‴) are the equivalent 9,10-conformations for 8,9-conformation (E). The relative populations of these conformations were not derived.

Conformations of the 11,12-*bond.* Although segmental motion[10] imparts considerable freedom of motion to the side-

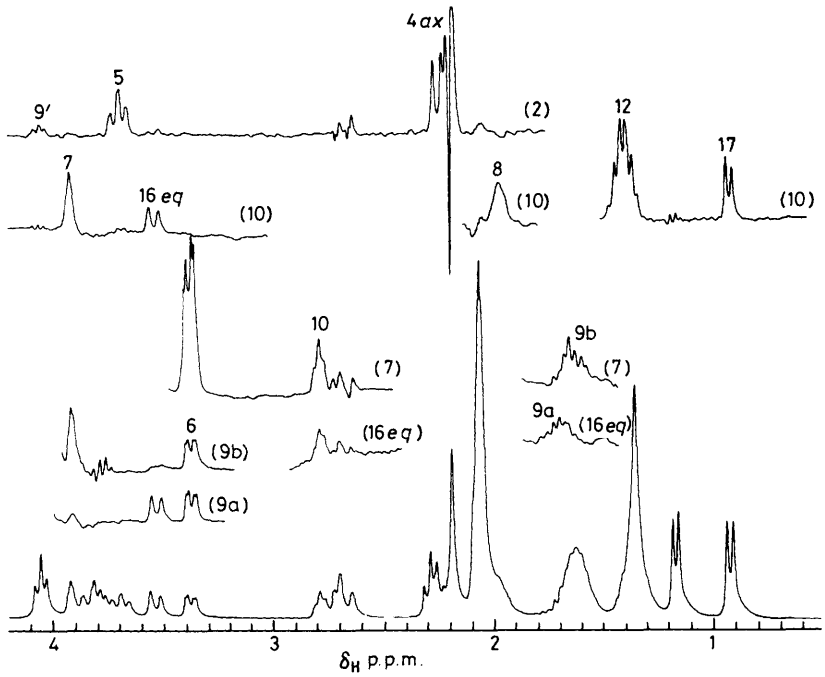

Figure 3. A control 250 MHz ^{1}H n.m.r. spectrum of pseudomonic acid A in [$^2H_6$]acetone underneath a series of n.O.e. difference spectra. The numbers in parentheses indicate the protons irradiated; the numbers without parentheses are signal assignments

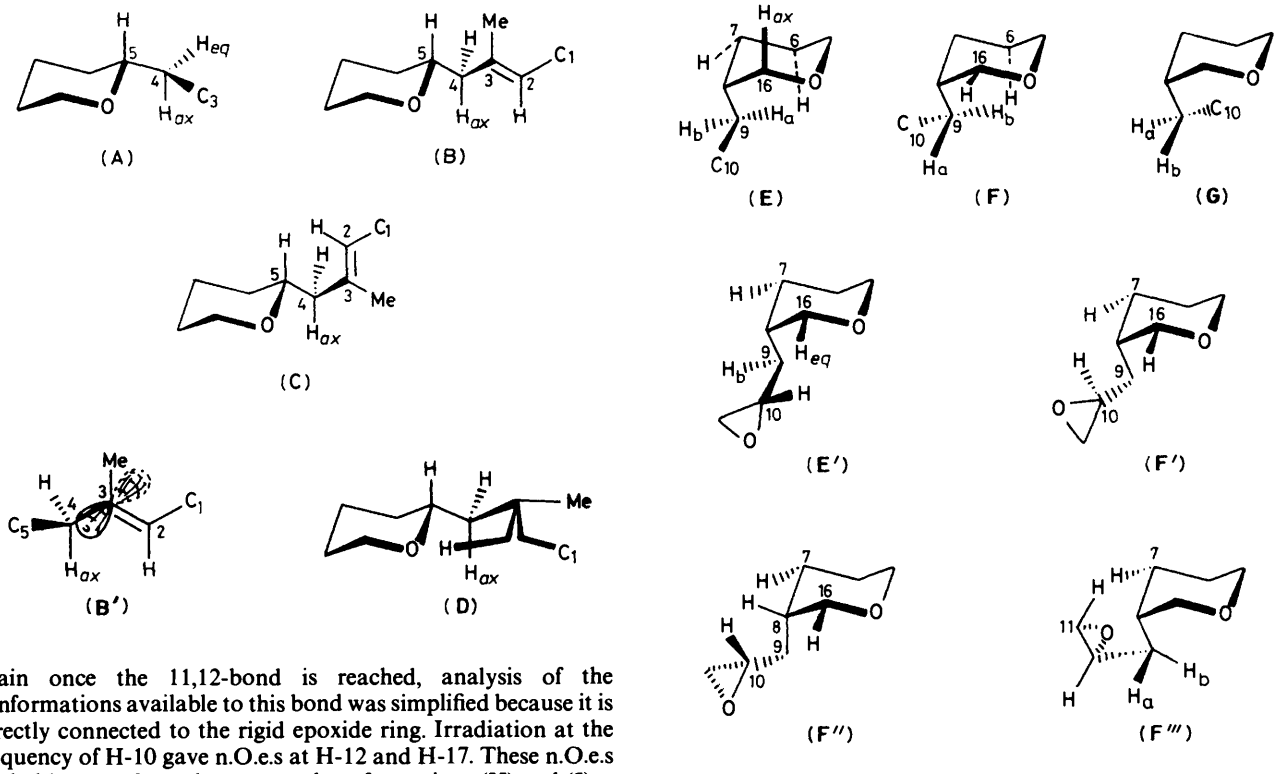

chain once the 11,12-bond is reached, analysis of the conformations available to this bond was simplified because it is directly connected to the rigid epoxide ring. Irradiation at the frequency of H-10 gave n.O.e.s at H-12 and H-17. These n.O.e.s probably arose from the staggered conformations (H) and (J).

The 10-proton is close to H-12 in (J) and to 17-H_3 in (H). If the third rotamer (K) is populated at all then 14-H_3 and H-13 are pointed away from C-10 since no n.O.e.s to these protons were seen. It was not possible to distinguish between lack of population of (K) and population of (K) with severe restriction on the rotation of the 12,13-bond.

Irradiation at the frequency of 17-H_3 gave n.O.e.s at H-10 (H) and H-11 (J).

Other n.O.e. results. Irradiation at the frequency of 14-H_3 gave an n.O.e. at H-11 but not at H-10. Thus in the manifold of conformations available to the C-14 methyl group there is one with close approach to H-11 but none with close approaches to H-10.

Irradiation at the frequency of H-2 gave a very small n.O.e. at H-9'. Thus in the manifold of conformations available to the C-9' methylene group there is one with a close approach to H-2.

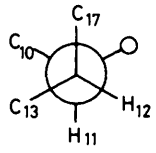

(H)

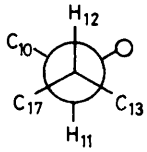

(J)

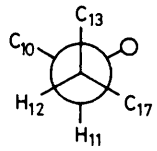

(K)

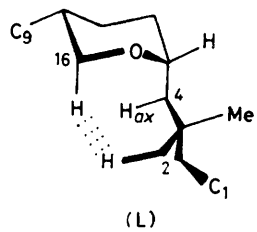

(L)

Summary of results for pseudomonic acid A. Pseudomonic acid A (**1**) in [$^2H_6$]acetone adopts a variety of conformations, all of which are in equilibrium. The thp ring adopts a *C*1 conformation. The 4,5-bond adopts a staggered conformation (A) with H-4*eq trans* to the thp oxygen. The 3,4-bond adopts two conformations (B) and (C) with the former more populated. The 8,9-bond adopts two staggered conformations (E) and (F) with the former more populated. The 9,10-bond adopts three staggered conformations, (E′), (E″), (E‴), (F′), (F″), (F‴), for each of the staggered conformations of the 8,9-bond. The 11,12-bond adopts at least two [(H), (J)] of the three [(H), (J), (K)] possible staggered conformations available to it.

The Conformations of Monic Acid in [$^2H_6$]*Acetone.*—Monic acid A (**3**) is antibacterially inactive and it was of interest to compare its conformations with those of (**1**).

The magnitudes of $^3J_{5,6}$ (9.2), $^3J_{6,7}$ (3.2), $^3J_{7,8}$ (3.2), $^3J_{16eq,8}$ (1.8), and $^3J_{16ax,8}$ (2.7 Hz) indicated that the thp ring of (**3**) was predominantly in the *C*1 conformation, as for (**1**).

The values of $^3J_{5,4ax}$ (9.2) and $^3J_{5,4eq}$ (2.6 Hz) indicated that the 4,5-bond of (**3**) was in the same conformation (A) as in (**1**). The near-maximal value of the *trans* coupling $^3J_{5,4ax}$ indicated little freedom of rotation around this bond.

The observation of n.O.e.s from H-2 to H-5 (0.5%) and H-4*ax* (1.9%) indicated that there were two conformations around the 3,4-bond, one with H-2 close to H-5 (minor) and one with H-2 close to H-4*ax* (major) as for (**1**). The major-to-minor conformer ratio was greater for (**3**) than (**1**), however. The observation of three long-range couplings $^4J_{4eq,15}$ (*ca.* 0.4), $^4J_{2,4eq}$ (1.3), and $^4J_{2,4ax}$ (*ca.* 0.85 Hz) indicated that these major and minor conformations were equivalent to (B) and (C), respectively.

The observation of $^4J_{16ax,9b}$ and an n.O.e. between H-7 and H-9b (1.4%) indicated that conformations like (E) were populated. Further, an n.O.e. was observed between H-7 and H-10 (*ca.* 0.5%), indicating that (F) was also populated. Overall, the conformations of (**3**) were very similar to those of (**1**) in [$^2H_6$]acetone, with the exception of the slightly greater ratio of major-to-minor conformers about the 3,4-bond in (**3**).

The Conformations of Sodium Pseudomonate A in D_2O.—Pseudomonic acid A (**1**) is only sparingly soluble in water and therefore the sodium salt (**2**) was studied in D_2O to determine whether or not the conformations were different in this biologically more realistic medium.

The spectra of (**2**) in D_2O showed differences from those of (**1**) in [$^2H_6$]acetone. The value of $^3J_{5,6}$ (8.0) was low, that of $^3J_{6,7}$ (3.1) the same, and those of $^3J_{16eq,8}$ (3.4) and $^3J_{7,8}$ (4.5 Hz) were high relative to the equivalent values for (**1**) in [$^2H_6$]acetone. These results indicated that the thp ring conformation was a mixture of *C*1 (*ca.* 80%) and *C*2 (*ca.* 20%).

The mixing of *C*2 with *C*1 causes a lowering of $^3J_{5,6}$ (*eq,eq* mixed with *ax,ax*), a raising of $^3J_{7,8}$ and $^3J_{8,16eq}$ (*ax,ax* mixed with *eq,eq*) and no effect on $^3J_{6,7}$ (*eq,ax* mixed with *ax,eq*). Confirmation of the existence of the *C*2 conformation came from the observation of an n.O.e. from H-2 to H-16*eq* (0.4%). The 4,5-bond was rigidly held ($^3J_{5,4ax}$ 9.9, $^3J_{5,4eq}$ 2.8 Hz), as in (**1**). The 3,4-bond populates the same two conformations (B) and (C) as in (**1**) [n.O.e. from H-2 to H-5 (1.5%) and H-4*ax* (1.6%), $^4J_{2,4ax}$ 0.6, $^4J_{2,4eq}$ 1.1 Hz, and $^4J_{15,4eq}$ broadening], the only difference being the lower ratio of the major-to-minor conformations. Thus in the major 3,4-bond conformation of *C*2 (L), H-2 is very close to H-16*eq* (which is now actually axial!) and an n.O.e. is observed between the two protons.

This is the first time that evidence for the existence of the thp ring-inverted *C*2 conformation has been obtained in this system. There was no sign of a W coupling between H-16*ax* and either H-9a or H-9b in (**2**). However, (**2**) populates conformations equivalent to (E) and (F), since irradiation at the frequency of H-9b (δ 1.79) gave n.O.e.s at H-7 [0.9%, (E)], H-6 [0.8%, (F)], and H-11 (1.1%). Irradiation at the frequency of H-9a (*ca.* δ 1.65) gave n.O.e.s at H-16*eq* and H-6 [1.4% total, (E) + (F)] and H-11 (1.6%). However, in (**2**) H-9b resonates downfield of H-9a and not upfield as in (**1**).

Thus, in general, (**2**) in D_2O adopts similar conformations to (**1**) in [$^2H_6$]acetone except that (**2**) populates the *C*2 thp ring conformation (*ca.* 20%) and has a slightly lower ratio of conformers about the 3,4-bond.

The Conformations of Monic Acid in D_2O.—The study of monic acid A (**3**) in D_2O was conducted in order to determine if there were any conformational differences between (**3**) (antibacterially inactive) and sodium pseudomonate A (**2**) (antibacterially active) in a biologically realistic medium.

The thp ring existed in both conformations *C*1 (*ca.* 80%) and *C*2 (*ca.* 20%). The pertinent data are: $^3J_{5,6}$ *ca.* 8.2, $^3J_{6,7}$ *ca.* 3.2, $^3J_{7,8}$ *ca.* 4.5, and $^3J_{16eq,8}$ *ca.* 3.2; irradiation at the frequency of H-2 gave an n.O.e. at H-16*eq* (*ca.* 0.5%). The 4,5-bond is rigidly held in the same conformation (A) as in (**2**), with $^3J_{5,4ax}$ *ca.* 10.2 and $^3J_{5,4eq}$ *ca.* 2.5 Hz. Irradiation at the frequency of H-2 gave n.O.e.s at H-5 [1.7%, (C)], H-4*ax* [2.6%, (B)], and H-4*eq* (small and negative due to transfer of n.O.e. from H-4*ax*).[4] Irradiation at the frequency of H-9b (δ 1.80) gave n.O.e.s at H-7 [1.0%, (E)], H-6 [1.0%, (F)], and H-11 (1.0%). Irradiation at the frequency of H-9a (δ 1.65) gave n.O.e.s at H-6 and H-16*eq* [1.7% total, (E) and (F)] and H-11 (1.5%). Irradiation at the frequency of H-10 gave n.O.e.s at H-7 [1.4%, (F′)], H-16*eq* [0.7%, (E′)], H-8 [*ca.* 1%, (F″), (E″)], H-12 [5.4%, (J)], and H-17 [1.3%, (H)].

Thus the conformations of (**3**) in D_2O were very similar to those of (**2**) in D_2O except that the ratio of conformations (B) to (C) about the 3,4-bond was slightly lower in (**2**). This is similar to the difference between (**1**) and (**3**) in [$^2H_6$]acetone. There is a total loss of antibacterial activity in going from pseudomonic acid A to monic acid A. Since the two molecules have similar conformations in [$^2H_6$]acetone and D_2O, the loss in activity may be ascribed to the removal of the nonanoic acid side-chain itself rather than any resultant conformational changes in the monate part of the molecule.

A Comparison between Solution-state and Crystalline-state Conformations.—*X*-Ray crystal structures are often used as models for the solution conformations of drug molecules. In particular, crystal structures are often used in computer graphics as the starting points for energy-minimisation calculations on related and possibly as yet unsynthesized

Table 2. Comparison of solution and crystal conformations

	Solution		Crystal		
Conformation	(1)[a]	(2)[b]	(X)[d]	(Y)[e]	(Z)[f]
thp ring	*C*1	*C*1/*C*2	*C*1	*C*1	*C*1
4,5-Bond	(A)	(A)	(A)	(A)	(A)
3,4-Bond	(B)/(C)	(B)/(C)	(C)	(C)	
8,9-Bond	(E)/(F)	(E)/(F)	(E)	(E)	(E)
9,10-Bond	(E′)(E″)(E‴) (F′)(F″)(F‴)	*c*	(E′)		(E″)

[a] [$^2H_6$]Acetone solution. [b] D_2O solution. [c] Thought to be the same as (1). [d] Ethyl 2-fluoromonate A. [e] Ethyl monate C. [f] Hydrazone of the nuclear ketone.

compounds. It was therefore of considerable interest to compare the solution and crystal conformations of pseudomonic acid A. This objective was immediately thwarted as no crystal structure of (1) is available. The closest derivative for which the crystal structure has been solved is ethyl 2-fluoromonate A.[12] Crystal structures have also been reported for ethyl monate C[13] and a hydrazone of the nuclear ketone.[3]

All three crystal structures showed a *C*1 thp ring conformation, an (A) 4,5-bond conformation, a (C) 3,4-bond conformation (except for the hydrazone which is not comparable), and an (E) 8,9-bond conformation. Table 2 compares these crystal conformations with the solution conformations for (1) and (2).

In solution, (1)—(3) have, or have as the major component, these thp and 4,5-bond conformations. However, in solution the (C) conformation is the minor 3,4-bond conformation. For (1) and (3) in [$^2H_6$]acetone the major 8,9-bond conformation is (E), as in the crystalline state for the related compounds. The populations of (E) and (F) are unknown for (2) and (3) in D_2O. In ethyl 2-fluoromonate A the 9,10-bond was in the (E′) conformation whereas in the hydrazone it was in the (E″) conformation. In solution (1) was shown to populate both these conformations as well as (F′), (F″), (F‴), and (E‴).

In summary, all the conformational features found in the crystalline state were also found in solution. However, many solution conformations were found which were not represented in the crystalline state. In terms of the biological action of a drug it is the solution state which is of prime importance. N.m.r. spectroscopy thus has two major advantages over *X*-ray crystallography in defining the conformations of a drug, in that n.m.r. spectroscopy operates in the solution state and is capable of identifying all available conformations, not just the one into which the molecule crystallises. Consequently there is a great potential for n.m.r. as well as *X*-ray data to be used as input for computer graphics studies of molecular shape.

Conclusions.—Detailed study of the proton n.m.r. spectrum of (1) in [$^2H_6$]acetone showed that the molecule exhibited a plethora of conformations. n.O.e.s were used to detect and identify these conformations. The only significant difference in [$^2H_6$]acetone between the conformations of (1) and those of the antibacterially inactive monic acid A (3) was that the ratio of conformers [(B) to (C)] around the 3,4-bond was slightly greater in (3). A similar difference was found between (3) and sodium pseudomonate A (2) in D_2O. Thus the lack of antibacterial activity in (3) was ascribed to the loss of the nonanoic acid side-chain rather than any resultant conformational changes. A survey of the crystalline-state conformations of three derivatives of (3) showed that they exhibited only a limited number of the conformational features found for (1)—(3) in solution. It is concluded that n.m.r. as well as *X*-ray data would make a valuable contribution to computer graphics calculations of molecular shape.

N.m.r. spectroscopy has been shown to be a powerful method for the investigation of the conformations of flexible drugs in solution. The ability to determine experimentally whether loss or gain of biological activity is due to conformational changes is very useful[14] in studies of structure–activity relationships.

Experimental

The 1D ^1H n.m.r. and 2D SECSY ^1H n.m.r. experiments were carried out at 250 MHz on a Bruker WM-250 instrument, using *ca.* 0.05M-solutions in 5 mm tubes, with tetramethylsilane as reference. The 2D SECSY experiment used N-type phase-cycling and a 45° mixing pulse (2 μs). Free induction decays (FIDs) were acquired over 1 024 data points and 1 400 Hz for each of 512 values of the evolution time. The second dimension (f1) sweep width was 480 Hz. The raw data were zero-filled in both dimensions to give a 1 024 × 2 048 matrix prior to double Fourier transformation. The n.O.e. difference spectra were acquired[4] using irradiation and relaxation times of 4 s each. The FIDs were line-broadened by 2 Hz prior to subtraction. All spectra of solutions in [$^2H_6$]acetone were acquired after removal of the exchangeable proton resonances by dissolution in CD_3OD and then evaporation to dryness prior to dissolving the samples in [$^2H_6$]acetone itself.

The 2D ^1H,^{13}C correlation n.m.r. spectrum was acquired at 400 MHz for ^1H on a Bruker WH-400 instrument, using a *ca.* 0.5M-solution in a 10 mm tube. Carbon-13 FIDs were acquired over 7 088 Hz and 2 048 points for each of 512 values of the evolution time. The proton (f1) sweep width was 1 110 Hz. The 90° proton pulse width was 30 μs and the 90° ^{13}C pulse width was 36 μs. The f2 data were zero-filled once prior to double Fourier transformation.

Acknowledgements

We thank Mr. M. Buckingham and Dr. L. Yan for the WH 400 spectrum and Dr. G. E. Hawkes (U.L.I.R.S.) for making n.m.r. facilities available. We also thank Mr. E. A. Cutmore for checking the manuscript and Dr. P. J. O'Hanlon for supplying authentic samples.

References

1 A. T. Fuller, G. Mellows, M. Woolford, G. T. Banks, K. D. Barrow, and E. B. Chain, *Nature*, 1971, **234**, 416.
2 Sir E. B. Chain and G. Mellows, *J. Chem. Soc., Perkin Trans. 1*, 1977, 294.
3 R. G. Alexander, J. P. Clayton, K. Luk, N. H. Rogers, and T. J. King, *J. Chem. Soc., Perkin Trans. 1*, 1978, 561.
4 J. K. M. Sanders and J. D. Mersh, *Prog. Nucl. Magn. Reson. Spectrosc.*, 1982, **15**, 353.
5 A. D. Bain, R. A. Bell, J. R. Everett, and D. W. Hughes, *J. Chem. Soc., Chem. Commun.*, 1980, 256.
6 A. D. Bain, R. A. Bell, J. R. Everett, and D. W. Hughes, *Can. J. Chem.*, 1980, **58**, 1947.
7 R. Freeman and G. Morris, *J. Chem. Soc., Chem. Commun.*, 1978, 684.
8 T. C. Feline, R. B. Jones, G. Mellows, and L. Phillips, *J. Chem. Soc., Perkin Trans. 1*, 1977, 309.
9 S. Sternhell, *Rev. Pure Appl. Chem.*, 1964, 15.
10 J. R. Everett and J. W. Tyler, *J. Antibiot.*, 1984, **37**, 363.
11 H. Booth, *Tetrahedron Lett.*, 1965, 411.
12 M. J. Crimmin, P. J. O'Hanlon, N. H. Rogers, and T. J. King, unpublished results.
13 J. P. Clayton, P. J. O'Hanlon, N. H. Rogers, and T. J. King, *J. Chem. Soc., Perkin Trans. 1*, 1982, 2827.
14 W. G. Richards, 'Quantum Pharmacology,' Oxford University Press, 1977.

Received 13*th August* 1984; *Paper* 4/1428